Triton calculations with π and ρ exchange three-nucleon forces

A. Stadler
Institut für Theoretische Physik, Universität Hannover, D-30167 Hannover 1, Germany
and
*Department of Physics, College of William and Mary, Williamsburg, Virginia 23185, U.S.A.**

J. Adam Jr.
Institute of Nuclear Physics, CZ-25068, Řež, Czech Republic

H. Henning, and P.U. Sauer
Institut für Theoretische Physik, Universität Hannover, D-30167 Hannover 1, Germany
(December 31, 2013)

arXiv:nucl-th/9504012v1 10 Apr 1995

Abstract

The Faddeev equations are solved in momentum space for the trinucleon bound state with the new Tucson-Melbourne π and ρ exchange three-nucleon potentials. The three-nucleon potentials are combined with a variety of realistic two-nucleon potentials. The dependence of the triton binding energy on the πNN cut-off parameter in the three-nucleon potentials is studied and found to be reduced compared to the case with pure π exchange. The ρ exchange parts of the three-nucleon potential yield an overall repulsive effect. When the recommended parameters are employed, the calculated triton binding energy turns out to be very close to its experimental value. Expectation values of various components of the three-nucleon potential are given to illustrate their significance for binding.

21.30.+y, 21.10.Dr, 21.45+v, 27.10.+h

Typeset using REVTEX

*Present address.

I. INTRODUCTION

None of the dynamical models for hadronic interactions that have been constructed in the past to microscopically describe nuclear properties is fundamental. All models are effective ones; only the most important hadronic degrees of freedom are taken into account explicitly. Effective theories in general lead to rather complicated forces, including irreducible many-body forces. The complexity and interpretation of these potentials is closely related to the chosen hadronic degrees of freedom. Most often the microscopic theory of nuclear phenomena is formulated in a Hilbert space of nucleons only employing nonrelativistic quantum mechanics. The potentials are taken to be of two-body nature, the mediating meson fields having been frozen out. Many-meson exchanges and relativistic effects are absorbed into the phenomenological short-range part of the potential that is also introduced to regularize it at the origin. Many-body forces are assumed to be much less important than the dominant two-nucleon force. This is a reasonable assumption, since on average nucleons move relatively slowly inside nuclei, three nucleons rarely interact simultaneously due to the short-range repulsion between two of them, and the rate of nucleonic excitation into nonnucleonic states is low. The parameters of these semi-phenomenological models are calibrated to reproduce the bound-state and scattering observables of the two-nucleon systems. Therefore, the three-nucleon system offers the first testing ground for the two-nucleon potentials. Can a Hamiltonian with only two-nucleon potentials successfully describe the trinucleon properties or not? The qualitative and quantitative effects of three-nucleon forces must be understood.

The derivation of realistic two-nucleon potentials has been steadily improved in the past. See the very good review of Ref. [1] on this subject. Furthermore, the techniques to solve the three-nucleon bound-state problem have reached maturity, the vast progress became possible by the rapid advances of computational power. The trinucleon calculations made it clear that no realistic two-nucleon potential is able to reproduce the known hadronic and e.m. properties of ^{3}H and ^{3}He with satisfactory accuracy. E.g., the triton binding energy obtained from such two-nucleon Hamiltonians turns out to be about 1 MeV below its experimental value. Calculations of ^{4}He show a similar deficiency in binding energy [2–4]. Thus, three-nucleon forces have to provide additional net attraction in order to close the gap between theoretical prediction for and experimental value of nuclear binding energies.

Two strategies for introducing three-nucleon forces have been investigated: In the first one a three-nucleon potential is designed to be added to a conventional Hamiltonian with two-nucleon potentials [5–9]. In the second one, the role of nucleonic excitation in generating three-nucleon forces is recognized: E.g., in Refs. [10,11] three-nucleon forces are obtained by the explicit inclusion of a Δ isobar in an extended Hilbert space. It came as a surprise that both strategies yield rather different trinucleon binding energies, even when the underlying physical processes are thought to be comparable. An attempt to combine the two approaches has been made in Ref. [13] where also their respective advantages and disadvantages are discussed. The present paper reports on triton calculations with a new three-nucleon force [14] that belongs to the first strategy.

Like all modern realistic two-nucleon potentials, the models for a three-nucleon force are based on meson exchange. Since nucleons are kept apart by short-range two-nucleon repulsion, the two-pion ($\pi\pi$) exchange part of the three-nucleon force is expected to be

dominant. Several $\pi\pi$ exchange three-nucleon potentials have been worked out. When used in triton calculations they provide ample additional binding energy. However, in contrast to expectation, its effect is strongly dependent on the cut-off parameter $\Lambda_{\pi NN}$ entering the regularizing form factor at the πNN vertices, i.e., it is dependent on non-pion physics. These purely phenomenological form factors are usually taken either in monopole or in square root parametrization. Since the same vertex also enters all models of the two-nucleon and the pion-nucleon potentials, both nucleon-nucleon and pion-nucleon scattering have been used to extract the value of the cut-off parameter $\Lambda_{\pi NN}$. Unfortunately, the answer is not unique. The two-nucleon potentials seem to demand "hard" form factors with a $\Lambda_{\pi NN}$ of about 1.2 GeV, whereas the analysis of πN scattering favors "soft" ones with $\Lambda_{\pi NN}$ typically around 800 MeV (for a discussion see [15]). When such a soft form factor is employed in a $\pi\pi$ exchange three-nucleon potential, the triton turns out to be already overbound. Further increase of $\Lambda_{\pi NN}$ leads to unphysically large binding energies well before $\Lambda_{\pi NN}$ reaches the characteristic values for hard form factors.

It is well known from two-nucleon potentials that the exchange of a ρ meson cancels to some extent the medium range part of the one-pion exchange tensor force, providing an important medium range repulsion to the two-nucleon potential. This cancellation also reduces the cut-off dependence of the two-nucleon potential. Thus, the inclusion of ρ exchange into three-nucleon force models should lead to less cut-off dependent results and simultaneously to a smaller overall contribution of the three-nucleon force to the triton binding energy. In the context of strategy 2 for the three-nucleon force this hope was confirmed already a long time ago [12].

The $\pi\rho$ and $\rho\rho$ contributions to three-nucleon potentials were derived already in [16–18,9]. Due to the enormous technical difficulties it is only now that they are being included in exact triton calculations. First results with the Brazilian three-nucleon potential were presented in Ref. [19]. They display the desired repulsive effect of the ρ exchange on the triton binding, but do not study its cut-off dependence, since the authors were only interested in determining parameter combinations that fit the experimental three-nucleon binding energy. Recently, Coon and Peña [14] reexamined and improved the $\pi\rho$ and $\rho\rho$ exchange three-nucleon potential [16] that was developed by the Tucson-Melbourne group as an extension of their $\pi\pi$ exchange three-nucleon potential [5].

In this paper we report our results of Faddeev calculations in momentum space for the triton binding energy, where the family of π and ρ exchange Tucson-Melbourne three-nucleon potentials is employed. In Section II the explicit expressions of these potentials are given. In Section III the numerical results are displayed and discussed, followed by a summary in Section IV.

II. THE TUCSON-MELBOURNE THREE-NUCLEON POTENTIALS

The full Tucson-Melbourne $\pi\rho$ and $\rho\rho$ exchange potentials are given in Ref. [14]. We do not comment on the physical origin of the various contributions but just display the final expressions in momentum space. For completeness we also include the $\pi\pi$ exchange part. We take over the notation of Ref. [16]. For the definition of the various occurring momenta see Figs. 1-3, where the basic diagrams of the three-nucleon potentials are shown.

The three-nucleon potentials in momentum space read

$$\langle \mathbf{k}_1' \mathbf{k}_2' \mathbf{k}_3' | W | \mathbf{k}_1 \mathbf{k}_2 \mathbf{k}_3 \rangle = \sum_{\alpha\beta=\pi,\rho} \sum_{i=1}^{3} \langle \mathbf{k}_1' \mathbf{k}_2' \mathbf{k}_3' | W_i^{\alpha\beta} | \mathbf{k}_1 \mathbf{k}_2 \mathbf{k}_3 \rangle, \tag{1}$$

$$\begin{aligned}
&\langle \mathbf{k}_1' \mathbf{k}_2' \mathbf{k}_3' | W_1^{\pi\pi} | \mathbf{k}_1 \mathbf{k}_2 \mathbf{k}_3 \rangle = \frac{1}{(2\pi)^6} \frac{\delta(\mathbf{k}_1' + \mathbf{k}_2' + \mathbf{k}_3' - \mathbf{k}_1 - \mathbf{k}_2 - \mathbf{k}_3)}{(\mathbf{q}^2 + \mu^2)(\mathbf{q}'^2 + \mu^2)} R^{\pi\pi}(\mathbf{q}^2, \mathbf{q}'^2) \\
&\times (\boldsymbol{\sigma}_2 \cdot \mathbf{q})(\boldsymbol{\sigma}_3 \cdot \mathbf{q}') \left\{ (\boldsymbol{\tau}_2 \cdot \boldsymbol{\tau}_3) \left[a + b \mathbf{q} \cdot \mathbf{q}' + c(\mathbf{q}^2 + \mathbf{q}'^2) \right] + (i \boldsymbol{\tau}_1 \cdot \boldsymbol{\tau}_2 \times \boldsymbol{\tau}_3) d (i \boldsymbol{\sigma}_1 \cdot \mathbf{q} \times \mathbf{q}') \right\} ,
\end{aligned} \tag{2}$$

$$\begin{aligned}
&\langle \mathbf{k}_1' \mathbf{k}_2' \mathbf{k}_3' | W_1^{\pi\rho} | \mathbf{k}_1 \mathbf{k}_2 \mathbf{k}_3 \rangle = -\frac{1}{(2\pi)^6} \frac{\delta(\mathbf{k}_1' + \mathbf{k}_2' + \mathbf{k}_3' - \mathbf{k}_1 - \mathbf{k}_2 - \mathbf{k}_3)}{(\mathbf{q}^2 + m_\rho^2)(\mathbf{q}'^2 + \mu^2)} (\boldsymbol{\sigma}_3 \cdot \mathbf{q}') \\
&\times \Big\{ -(i \boldsymbol{\tau}_1 \cdot \boldsymbol{\tau}_2 \times \boldsymbol{\tau}_3) R_{KR}^{\pi\rho}(\mathbf{q}^2, \mathbf{q}'^2) (i \boldsymbol{\sigma}_1 \cdot \boldsymbol{\sigma}_2 \times \mathbf{q}) \\
&\quad + (\boldsymbol{\tau}_2 \cdot \boldsymbol{\tau}_3) R_{\Delta^+}^{\pi\rho}(\mathbf{q}^2, \mathbf{q}'^2) (\mathbf{q} \times \mathbf{q}') \cdot (\mathbf{q} \times \boldsymbol{\sigma}_2) \\
&\quad + (i \boldsymbol{\tau}_1 \cdot \boldsymbol{\tau}_2 \times \boldsymbol{\tau}_3) R_{\Delta^-}^{\pi\rho}(\mathbf{q}^2, \mathbf{q}'^2) \left[(i \boldsymbol{\sigma}_1 \cdot \boldsymbol{\sigma}_2 \times \mathbf{q}') \mathbf{q}^2 - (i \boldsymbol{\sigma}_1 \cdot \mathbf{q} \times \mathbf{q}') (\boldsymbol{\sigma}_2 \cdot \mathbf{q}) \right] \Big\} \\
&\qquad + (2 \leftrightarrow 3 \,, \qquad \mathbf{q} \leftrightarrow -\mathbf{q}') \,,
\end{aligned} \tag{3}$$

and

$$\begin{aligned}
&\langle \mathbf{k}_1' \mathbf{k}_2' \mathbf{k}_3' | W_1^{\rho\rho} | \mathbf{k}_1 \mathbf{k}_2 \mathbf{k}_3 \rangle = -\frac{1}{(2\pi)^6} \frac{\delta(\mathbf{k}_1' + \mathbf{k}_2' + \mathbf{k}_3' - \mathbf{k}_1 - \mathbf{k}_2 - \mathbf{k}_3)}{(\mathbf{q}^2 + m_\rho^2)(\mathbf{q}'^2 + m_\rho^2)} \\
&\times \Big\{ (i \boldsymbol{\tau}_1 \cdot \boldsymbol{\tau}_2 \times \boldsymbol{\tau}_3) R_{Beg}^{\rho\rho}(\mathbf{q}^2, \mathbf{q}'^2) i \boldsymbol{\sigma}_1 \cdot (\boldsymbol{\sigma}_2 \times \mathbf{q}) \times (\boldsymbol{\sigma}_3 \times \mathbf{q}') \\
&\quad + (\boldsymbol{\tau}_2 \cdot \boldsymbol{\tau}_3) R_{\Delta^+}^{\rho\rho}(\mathbf{q}^2, \mathbf{q}'^2) \left[(\boldsymbol{\sigma}_2 \times \mathbf{q}) \times \mathbf{q} \cdot (\boldsymbol{\sigma}_3 \times \mathbf{q}') \times \mathbf{q}' \right] \\
&\quad + (i \boldsymbol{\tau}_1 \cdot \boldsymbol{\tau}_2 \times \boldsymbol{\tau}_3) R_{\Delta^-}^{\rho\rho}(\mathbf{q}^2, \mathbf{q}'^2) i \boldsymbol{\sigma}_1 \cdot \left[((\boldsymbol{\sigma}_2 \times \mathbf{q}) \times \mathbf{q}) \times ((\boldsymbol{\sigma}_3 \times \mathbf{q}') \times \mathbf{q}') \right] \Big\} \,.
\end{aligned} \tag{4}$$

The following shorthands have been used in (2), (3), and (4):

$$R^{\pi\pi}(\mathbf{q}^2, \mathbf{q}'^2) = \frac{g^2}{4m^2} F_{\pi NN}^2(\mathbf{q}^2) F_{\pi NN}^2(\mathbf{q}'^2) \,, \tag{5}$$

$$R_{KR}^{\pi\rho}(\mathbf{q}^2, \mathbf{q}'^2) = \frac{g_\rho^2}{16m^3} \left[F_{\rho NN_D}(\mathbf{q}^2) + \kappa_\rho F_{\rho NN_P}(\mathbf{q}^2) \right] F_{\rho NN_D}(\mathbf{q}^2) g^2 F_{\pi NN}^2(\mathbf{q}'^2) \,, \tag{6}$$

$$\begin{aligned}
R_{\Delta^+}^{\pi\rho}(\mathbf{q}^2, \mathbf{q}'^2) &= \frac{g_\rho}{48m^5} \left[F_{\rho NN_D}(\mathbf{q}^2) + \kappa_\rho F_{\rho NN_P}(\mathbf{q}^2) \right] \\
&\quad \times G_{M\rho}^* F_{\rho N\Delta}(\mathbf{q}^2) \frac{m}{M} \frac{5M - m}{M - m} \left[m g^* F_{\pi N\Delta}(\mathbf{q}'^2) \right] F_{\pi NN}(\mathbf{q}'^2) \,,
\end{aligned} \tag{7}$$

$$R_{\Delta^-}^{\pi\rho}(\mathbf{q}^2, \mathbf{q}'^2) = \frac{1}{4} R_{\Delta^+}^{\pi\rho}(\mathbf{q}^2, \mathbf{q}'^2) \,, \tag{8}$$

$$\begin{aligned}
R_{Beg}^{\rho\rho}(\mathbf{q}^2, \mathbf{q}'^2) &= \frac{g_\rho^4}{64m^3} \left[F_{\rho NN_D}(\mathbf{q}^2) + \kappa_\rho F_{\rho NN_P}(\mathbf{q}^2) \right] \\
&\quad \times \left[F_{\rho NN_D}(\mathbf{q}'^2) + \kappa_\rho F_{\rho NN_P}(\mathbf{q}'^2) \right] \left[1 + \tilde{\kappa}_\rho(0) \right] F_{\rho NN_D}^2(0) \,,
\end{aligned} \tag{9}$$

$$R^{\rho\rho}_{\Delta^+}(\mathbf{q}^2,\mathbf{q}'^2) = \frac{g_\rho^2\lambda_M^2}{18(M-m)}\left[F_{\rho NN_D}(\mathbf{q}^2)+\kappa_\rho F_{\rho NN_P}(\mathbf{q}^2)\right]$$
$$\times F_{\rho N\Delta}(\mathbf{q}^2)\left[F_{\rho NN_D}(\mathbf{q}'^2)+\kappa_\rho F_{\rho NN_P}(\mathbf{q}'^2)\right]F_{\rho N\Delta}(\mathbf{q}'^2)\,, \tag{10}$$

$$R^{\rho\rho}_{\Delta^-}(\mathbf{q}^2,\mathbf{q}'^2) = \frac{1}{4}R^{\rho\rho}_{\Delta^+}(\mathbf{q}^2,\mathbf{q}'^2)\,, \tag{11}$$

with $\tilde{\kappa}_\rho(0)=3.7$ and $\lambda_M=-\frac{3}{2m(M+m)}G^*_{M\rho}$, where μ, m_ρ, m, and M denote the pion, the rho, the nucleon, and the Δ mass respectively.

Note that the potentials (2) – (4) represent only the part of the full force in which particle 1 interacts both with particles 2 and 3 (see Figs. 1-3). The other two contributions with particles 2 and 3 in the middle of the diagrams are obtained by permutations. The potentials are given as operators in the three-nucleon spin and isospin space. The employed three-nucleon basis states are normalized as

$$\langle \mathbf{k}'_1\mathbf{k}'_2\mathbf{k}'_3|\mathbf{k}_1\mathbf{k}_2\mathbf{k}_3\rangle = \delta(\mathbf{k}'_1-\mathbf{k}_1)\delta(\mathbf{k}'_2-\mathbf{k}_2)\delta(\mathbf{k}'_3-\mathbf{k}_3)\,. \tag{12}$$

The general structure of the regularization form factors F_i at the meson-baryon-baryon vertices is taken to be of monopole form, i.e.,

$$F_i(\mathbf{q}^2) = \frac{\Lambda_i^2-m_b^2}{\Lambda_i^2+\mathbf{q}^2}\,, \tag{13}$$

with $i=\{\pi NN,\pi N\Delta,\rho NN_D,\rho NN_P,\rho N\Delta\}$ and m_b the mass of the boson at the vertex (i.e., m_b is either μ or m_ρ; an exception is the case $i=\rho N\Delta$, where $m_b=0$), $F_{\rho NN_D}$ being the Dirac and $F_{\rho NN_P}$ the Pauli form factor. The numerical values of the employed masses and potential parameters are given in Table I. Note that the values of our parameters a, b, and c, are taken from Refs. [5,6] and differ slightly from those of Ref. [14]. The latter have been extracted from an updated set of experimental πN data and were published only after most of our numerical calculations have been completed (a short account of our results appeared in Ref. [20], where unfortunately the $\rho\rho$ part of the three-nucleon force was treated incorrectly).

Furthermore, the original [16] factor of $\frac{1}{4}$ in Eq. (8) has been changed in Ref. [14] to $\frac{1}{2}\frac{M+m}{5M-m}$ which numerically is approximately $\frac{1}{4.8}$ and also represents only a small variation. Both changes do not appear significant enough to justify repeating our very elaborate computations carried out prior to Ref. [14]. However, we have checked numerically that their net effect in the triton binding energy is small. More details can be found in Section III.

III. RESULTS

The Faddeev equations for the three-nucleon bound state with the inclusion of an irreducible three-nucleon force can be written as [21]

$$|\psi_i\rangle = G_0(E)\left\{T_i(E)P + \left[1+T_i(E)G_0(E)\right]W_i(1+P)\right\}|\psi_i\rangle\,, \tag{14}$$

where $|\psi_i\rangle$ is the Faddeev amplitude, $G_0(E)$ the free three-nucleon propagator, $T_i(E)$ the two-nucleon transition matrix embedded in the three-nucleon Hilbert space, W_i the potential operator of the irreducible three-nucleon force, and P the sum of the two operators for cyclic and anticyclic permutations of the three particles. The subscript i denotes in $|\psi_i\rangle$ and $T_i(E)$ the spectating particle, and in W_i the particle that interacts simultaneously with the other two. E is the the trinucleon binding energy. Equation (14) is employed in momentum space and expanded into partial waves. The explicit form of the resulting set of coupled integral equations in two continuous variables as well as details of the solution method have been presented in Ref. [21]. All results of this section were obtained in a basis of 18 partial waves. They correspond to all possible combinations of spin-, isospin- and orbital angular-momentum quantum numbers that can be coupled to the quantum numbers of the triton, when the two-nucleon pair interaction is restricted to total angular momenta up to 2.

The main difficulty of this work as an extension of Ref. [21] was the partial wave decomposition of the $\pi\rho$ and $\rho\rho$ exchange three-nucleon potentials, since their structure is considerably more complex than that of the $\pi\pi$ exchange potential. This complexity calls for a systematic procedure to decompose general three-nucleon operators into partial waves. Such a procedure was developed by Adam and Henning [22,23] and is applied in this work for the particular case of the Tucson-Melbourne three-nucleon potentials. Given the matrix elements of the three-nucleon potentials in partial wave decomposed form, their numerical evaluation is still a formidable task. In order to illustrate the enormous computing resources necessary for performing such calculations we note that the computation of the $\pi\pi$ exchange potential matrix elements in 18 channels on a Siemens/Fujitsu S400 Supercomputer, as it was done for Ref. [21], took about 90 minutes of CPU time. Therefore it was absolutely inevitable to develop a new method that exploits both the advantages of the general technique for multipole decomposition and the possibilities of efficient vectorization as much as possible. With that new method, the $\pi\pi$ exchange matrix elements are calculated within 3.5 minutes, the $\pi\rho$ exchange matrix elements within 10 minutes, and the $\rho\rho$ exchange matrix elements within 15 minutes of CPU time. The accuracy of the new code was tested by comparing $\pi\pi$ exchange potential matrix elements with results from the old technique and was found to be improved, too. Triton binding energies including the effect of $\pi\pi$ exchange three-nucleon potentials calculated with the old and the new codes agree.

Now we turn to the presentation of the triton binding energies obtained with the Tucson-Melbourne three-nucleon potentials.

In Table II the results for the Reid soft core [24], Paris [25], Nijmegen [26], and Bonn OBEPQ [27] as underlying two-nucleon potentials are given. We consider these potentials as representative for various approaches to modeling the two-nucleon force: they are purely phenomenological, based on dispersion theory, non-relativistic and derived from one-boson exchange, and derived from one-boson exchange with minimal relativity, respectively.

The binding energies obtained with the complete π and ρ exchange Tucson-Melbourne three-nucleon potentials (which we hereafter shorthand as "full results") scatter closely around the experimental triton binding energy of -8.482 MeV. The only exception occurs in the case of the Bonn OBEPQ potential, which comes close to that value already without any three-nucleon force. The full result for the Paris potential happens to deviate from the experimental value by only 12 keV.

As expected, the $\pi\rho$ three-nucleon potential decreases the trinucleon binding energy,

compensating to a large extent the overbinding due to the $\pi\pi$ potential alone. We also observe that the $\rho\rho$ potential has only a small effect. For the Δ mediated three-nucleon force of the Hannover model, it was found already many years ago [12] that the $\pi\rho$ exchange weakens the attraction due to the $\pi\pi$ exchange and that the contribution of the $\rho\rho$ exchange is rather small. These findings are also in good qualitative agreement with the results obtained by Sasakawa *et al.* [19] for the simpler Brazilian three-nucleon potentials. However, we want to point out that the calculations of Ref. [19] were performed with a different two-nucleon potential, that they include only the Δ part of the $\rho\rho$ potential, and that the implemented functional form of the ρ form factors as well as the values of the ρ cut-off parameters are very different from ours. That the effect of the $\rho\rho$ potential in our calculations can be attractive or repulsive, depending on the employed two-nucleon potential, while Ref. [19] reports only repulsion, is therefore not inconsistent.

However, one should not take the impressive agreement of theoretical binding energies with experiment too seriously, even though no attempt was made to adjust any parameters of the three-nucleon potential in order to reproduce the experimental trinucleon binding energy. One should keep in mind that the exact values of the cut-off parameters Λ_i are not well determined, although some arguments have been given [14] favoring the set of parameters listed in Table I. In particular, the recommended value for the πNN vertex, $\Lambda_{\pi NN} = 5.8\mu \approx 810$ MeV, is based on an analysis of the Goldberger-Treiman relation [28]. The uncertainties associated with the extrapolation of the physical constants in the Goldberger-Treiman relation to their chiral-limit values are estimated in Ref. [14] to yield a "theoretical error bar" of about ± 200 MeV for $\Lambda_{\pi NN}$, an uncertainty which creates substantial variation in the calculated triton binding energy.

Since it is known already from previous studies with the $\pi\pi$ exchange three-nucleon force [29,30,21] that the results are strongly dependent on the cut-off $\Lambda_{\pi NN}$ it is certainly necessary to reexamine that dependence for the full three-nucleon force. Each full calculation still requiring enormous computational capacities, we had to restrict ourselves to a small number of combinations of the cut-off parameters. Nevertheless, the studied variation is sufficient to draw some qualitative conclusions.

The variation of $\Lambda_{\pi NN}$ is performed using the same values as before in the study of the $\pi\pi$ exchange three-nucleon force [30,21]. For the cut-off parameters connected with the ρ meson we consider just two cases, i.e., on one hand soft form factors, represented by the Tucson-Melbourne choice $\Lambda_{\rho NN_D} = 12.0\mu$ and $\Lambda_{\rho NN_P} = 7.4\mu$, and on the other hand hard form factors as suggested by Ref. [17], with $\Lambda_{\rho NN_D} = \Lambda_{\rho NN_P} = \Lambda_{\rho N\Delta} = 13.4\mu$. These two choices of ρ cut-off parameters have also been considered in Ref. [14].

The results with the Paris potential as two-nucleon potential are shown in Table III and in Figure 4. The strong dependence on $\Lambda_{\pi NN}$ is considerably reduced once the $\pi\rho$ part is added to the three-nucleon force, although the remaining dependence is still sizeable. Changing the ρ cut-off parameters from "soft" to "hard" values also alters the triton binding energy: The effect of the $\rho\rho$ part is significantly enhanced for hard form factors. It is repulsive and greater than 200 keV (for $\Lambda_{\pi NN} = 5.8\mu$), whereas it is less than 10 keV and attractive for soft form factors.

However, there are indications that the use of hard ρ cut-off parameters in the Tucson-Melbourne potential does not lead to physically meaningful results. Although our primary reference two-nucleon potential is the Paris potential, we repeated a calculation with hard

ρ cut-off parameters also for the Reid potential. We found that the $\rho\rho$ potential becomes so strong that no converged trinucleon binding energy could be obtained (for $\Lambda_{\pi NN} = 5.8\mu$). Apparently, there are strong and model-dependent cancellations between different components of the $\rho\rho$ potential which happen to reduce to a comparably small net result in the case of the Paris potential, while for other potentials they can diverge. A similar problem occurs already when only the $\pi\pi$ potential is considered: While stable trinucleon binding energies for the Reid and Paris potentials can be obtained when $\Lambda_{\pi NN} = 7.1\mu$, they diverge for Nijmegen or Bonn potentials.

We see two possible interpretations of these divergencies for hard cut-off parameters. Either the Tucson-Melbourne parametrization of the three-nucleon force is valid and there are physical reasons to favor soft form factors. Or the Tucson-Melbourne potentials are *mathematically* not well defined for hard form factors, i.e., in the course of solving the three-nucleon equations the Tucson-Melbourne potentials are evaluated outside their range of convergence associated with various Taylor expansions that are employed in their derivation. We believe it would be important to further investigate these questions. However, it is not the purpose of this paper, in which we rather want to focus on the original parametrization of the Tucson-Melbourne potentials.

The use of the updated parameters of the Tucson-Melbourne potential instead of the ones of Table I changes the triton binding energy by very little. The check was carried out by a complete recalculation for the entry -8.494 MeV under $\pi\pi + \pi\rho + \rho\rho$ soft with $\Lambda_{\pi NN} = 5.8\mu$ for the Paris potential in Table III. The updated parameters a, b, and c, in the $\pi\pi$ part of the three-nucleon potential change the triton binding energy from -8.494 MeV to -8.465 MeV. The subsequent modification of the factor $\frac{1}{4}$ in the isospin-odd Δ part of the $\pi\rho$ potential in (8) to the new prescription, discussed at the end of Sect. II, changes the value of -8.465 MeV to -8.492 MeV. Clearly, the found changes are small, in particular if compared to the sensitivity of the results to variations of the cut-off parameters.

Table IV lists expectation values of the various components of the Tucson-Melbourne three-nucleon potentials. These components are terms of different spin-, isospin-, and momentum dependence. In the $\pi\pi$ part of the three-mucleon potential they are labeled by their respective coefficients a, b, c, and d. In the case of the $\pi\rho$ and $\rho\rho$ potential they originate from distinct physical processes and are characterized accordingly as Δ, $K.R.$, and $Beg.$ Here Δ stands for the contributions originating from the Δ resonance, whereas $K.R.$ and Beg refer to the terms obtained from the Kroll-Ruderman and Bég low-energy theorems [16]. The superscripts $(\pm)$ indicate their isospin symmetry under particle exchange.

The expectation values are calculated with the fully correlated wave functions, i.e., they are obtained from the full Hamiltonian including the full three-nucleon potentials. They represent therefore true expectation values and not results from first order perturbation theory. In fact, a comparison of the expectation values with the corresponding binding energy differences demonstrates again the non-perturbative character of these calculations.

It can be seen that the unproportionally strong overbinding for the OBEPQ potential is mainly caused by the c-term of the $\pi\pi$ potential. There seems to be a correlation between the magnitudes of the expectation values and the probabilities of the wave function components. As one moves from left to right in Table IV, the triton D state probabilities decrease whereas the absolute values of the total $\pi\pi$, $\pi\rho$, and $\rho\rho$ contributions increase. The same trend holds also for most of the individual contributions.

In the $\pi\pi$ part of the three-nucleon potential, several physical processes lead to terms of the same spin-isospin and momentum structure. They are usually not separated in order to emphasize the model-independent character of the potential. However, it is interesting to see how the three-nucleon potential is composed of physical processes, even if a certain model dependence is introduced. In Ref. [14] the four coefficients of the $\pi\pi$ potential are split into different parts according to their physical origin. There, the given numerical values are based on the updated set of parameters. Since we are working with the original set of parameters, we have to recalculate this splitting accordingly. This is the reason why our values (16) are not identical to those of [14].

The coefficients are decomposed as

$$\begin{aligned} a &= a_\sigma \\ b &= b_\Delta + b_\sigma \\ c &= c_\sigma + c_Z \\ d &= d_\Delta + d_Z + d_{ca}\,, \end{aligned} \tag{15}$$

with the numerical values

$$\begin{aligned} a_\sigma &= 1.13\mu^{-1} \\ b_\Delta &= -1.676\mu^{-3}\,, \quad b_\sigma = -0.904\mu^{-3} \\ c_\sigma &= 1.15\mu^{-3}\,, \quad c_Z = -0.15\mu^{-3} \\ d_\Delta &= -0.36\mu^{-3}\,, \quad d_Z = -0.15\mu^{-3}\,, \quad d_{ca} = -0.243\mu^{-3}\,. \end{aligned} \tag{16}$$

The subscripts Δ, σ, and Z, refer to Δ-isobar, σ-term, and Z-graph contributions; ca is a "current algebra" term [14]. It represents a (isovector) vector-current contribution to the πN amplitude which the three-nucleon potential is based on. In a simple vector-meson dominance model it reduces to a t-channel ρ exchange part of the πN amplitude.

In this context it may be worth mentioning that not only the extraction of Δ contributions is model dependent, but also the separation into Z-graph and σ-term. In the Tucson-Melbourne πN amplitude, pure pseudoscalar πNN coupling is assumed. The separation into Z-graph and σ-term would change if pseudovector coupling were introduced.

The expectation values of Table IV are reorganized according to this analysis and displayed in Table V. The upper half contains only the results from the $\pi\pi$ potential, the lower half adds the respective pieces from the $\pi\rho$ and $\rho\rho$ potentials. The Kroll-Ruderman term is part of what is called Z-graph contributions, because as in the $\pi\pi$ potential pseudoscalar πNN coupling is assumed. The Bég term is counted as a "current algebra" contribution, since it originates from t-channel 3ρ and $\rho\rho NN$ contact terms. The σ-term appears only in the $\pi\pi$ potential. The corresponding expectation values are therefore identical in the upper and lower half of the table.

The Δ and σ-term contributions are both attractive and comparable in magnitude in the $\pi\pi$ potential. In the $\pi\rho$ potential, however, the Δ parts yield relatively strong repulsion, thus canceling to some extent the attraction they produce in the $\pi\pi$ potential. The Z-graph expectation values turn out to be small and repulsive, most of which is due to the Kroll-Ruderman term in the $\pi\rho$ potential. The current algebra term is similar in magnitude but

opposite in sign. Again, the results obtained with the OBEPQ potential take on rather extreme values. For the Paris potential, the expectation values of the Δ parts are quite similar to the ones obtained with the Δ mediated three-nucleon force presented in table 3 of Ref. [12].

IV. SUMMARY

We have solved the Faddeev equations with a new set of Tucson-Melbourne three-nucleon potentials, based on π and ρ exchange, together with realistic two-nucleon potentials for the three-nucleon bound state. We find that the $\pi\rho$ exchange three-nucleon potential is repulsive and counteracts the too strong attraction generated by the $\pi\pi$ potential to such an extent that the resulting triton binding energies for the Reid soft core, the Paris, and the Nijmegen potentials are close to the experimental value. This is not true for the Bonn OBEPQ potential which yields overbinding of more than 1 MeV. The strong dependence of the binding energy on the πNN vertex cutoff parameter $\Lambda_{\pi NN}$ that was observed for the Tucson-Melbourne $\pi\pi$ exchange three-nucleon potential is reduced once the ρ exchange is added. The $\rho\rho$ exchange potential has only a small effect on the triton binding energy as long as the vertex form factors are not chosen to be "hard".

We have calculated expectation values of the various components of the three-nucleon potentials. They are presented in two different ways: first they are grouped according to their spin-isospin and momentum dependence, and second they are rearranged to exhibit the relative strength of the underlying physical processes. We find that the contributions from the σ-term and from Δ excitations are dominant and attractive, compared to which the repulsive effect of intermediate Z-graphs is small. It is the σ-term part of the $\pi\pi$ potential that appears to be very sensitive to details of the three-nucleon wave function and that leads to the unusually strong overbinding in the case of the Bonn OBEPQ potential.

In the derivation of three-nucleon potentials, vertex functions are usually expanded in powers of particle momenta. The b, c, and d parts of the $\pi\pi$ potential are terms two orders higher in the pion momenta than the a term. The fact that they yield considerably larger expectation values in the triton might indicate a failure of the momentum expansion. Such a failure could simultaneously be responsible for the observed strong dependence on the π and ρ cut-off parameters.

That the effect of the $\pi\rho$ three-nucleon potential, although already much smaller than that of the $\pi\pi$ potential, is still of non-negligible size suggests that other exchange processes involving heavier mesons, such as $\pi\sigma$ and $\pi\omega$ exchange, should also be investigated. Since σ and ω exchange are included in most one-boson exchange two-nucleon potentials, they should also be included in three-nucleon potentials already for reasons of consistency. These processes have been found to be important in π production on two-nucleon systems at threshold (see, e.g., Ref. [31,32]).

We thank S. A. Coon and M. T. Peña for many helpful discussions on details of the Tucson-Melbourne three-nucleon potentials. This work was funded by the Deutsche Forschungsgemeinschaft (DFG) under the Contract Nos. Sa 247/7-2, Sa 247/7-3, Sa 247/9-4 and 436 CSR-111/4/90, and by the DOE under Grant No. DE-FG05-88ER40435. During part of the work, J. A. was fellow of the Humboldt Foundation. The calculations were

performed at Regionales Rechenzentrum für Niedersachsen (RRZN), Hannover, at Rechenzentrum Kiel, at Continuous Electron Beam Accelerator Facility (CEBAF), and at National Energy Research Supercomputer Center (NERSC), Livermore.

REFERENCES

[1] R. Machleidt, Adv. Nucl. Phys. **19**, 189 (1989).
[2] J. Carlson, Phys. Rev. C**38**, 1879 (1988).
[3] B. Wiringa, Phys. Rev. C**43**, 1585 (1991).
[4] W. Glöckle and H. Kamada, Phys. Rev. Lett. **71**, 971 (1993).
[5] S. A. Coon, M. D. Scadron, P. C. McNamee, B. R. Barrett, D. W. E. Blatt, and B. H. J. McKellar, Nucl. Phys. **A317**, 242 (1979).
[6] S. A. Coon and W. Glöckle, Phys. Rev. C**23**, 1790 (1981).
[7] M. R. Robilotta and H. T. Coelho, Nucl. Phys. **A460**, 645 (1986).
[8] T. Ueda, T. Sawada, T. Sasakawa, and S. Ishikawa, Prog. Theor. Phys. **72**, 860 (1984).
[9] S. Deister, M. F. Gari, W. Krümpelmann, and M. Mahlke, Few-Body Syst. **10**, 1 (1991).
[10] Ch. Hajduk and P. U. Sauer, Nucl. Phys. **A322**, 329 (1979).
[11] Ch. Hajduk, P. U. Sauer and W. Strueve, Nucl. Phys. **A405**, 581 (1983).
[12] Ch. Hajduk, P.U.Sauer, Shin Nan Yang, Nucl. Phys. **A405**, 605 (1983).
[13] A. Stadler and P. U. Sauer, Phys. Rev. C**46**, 64 (1992).
[14] S. A. Coon and M. T. Peña, Phys. Rev. C**48**, 2559 (1993).
[15] T. Ueda, Phys. Rev. Lett. **68**, 142 (1992); G. Jansen, J. W. Durso, K. Holinde, B. C. Pearce, and J. Speth, Phys. Rev. Lett. **71**, 1978 (1993); A. W. Thomas and K. Holinde, Phys. Rev. Lett. **63**, 2025 (1989).
[16] R. G. Ellis, S. A. Coon, and B. H. J. McKellar, Nucl. Phys. **A438**, 631 (1985).
[17] M. Martzolff, B. Loiseau, P. Grangé, Phys. Lett. **92B**, 46 (1980).
[18] M. R. Robilotta and M. A. Isidro Filho, Nucl. Phys. **A414**, 394 (1984).
[19] T. Sasakawa, S. Ishikawa, Y. Wu, and T-Y. Saito, Phys. Rev. Lett. **68**, 3503 (1992).
[20] A. Stadler, J. Adam Jr., H. Henning and P. U. Sauer, in *Conference Handbook of XIV European Conference on Few-Body Problems in Physics*, Amsterdam, 23-27 August, 1993, ed. L. P. Koch, pp. 192-193.
[21] A. Stadler, W. Glöckle, and P. U. Sauer, Phys. Rev. C**44**, 2319 (1991).
[22] H. Henning, J. Adam Jr., and P. U. Sauer, in preparation.
[23] H. Henning, Ph.D. thesis, in preparation.
[24] R. V. Reid, Ann. Phys. (N.Y.) **50**, 411 (1968).
[25] M. Lacombe, B. Loiseau, J. M. Richard, R. Vinh Mau, J. Côté, P. Pirès, and R. de Tourreil, Phys. Rev. C**21**, 861 (1980).
[26] M. M. Nagels, T. A. Rijken, and J. J. de Swart, Phys. Rev. D**17**, 768 (1978); T. A. Rijken, R. A. M. Klomp, and J. J. de Swart, Nijmegen preprint THEF-NYM-91.05.
[27] R. Machleidt, K. Holinde, and Ch. Elster, Phys. Rep. **149**, 1 (1987).
[28] S. A. Coon and M. D. Scadron, Phys. Rev. C**42**, 2256 (1990).
[29] T. Sasakawa and S. Ishikawa, Few-Body Syst. **1**, 3 (1986).
[30] C. R. Chen, G. L. Payne, J. L. Friar, and B. F. Gibson, Phys. Rev. C**33**, 1740 (1986).
[31] C. J. Horowitz, Phys. Rev. C**48**, 2920 (1993).
[32] T.-S. H. Lee and D. O. Riska, Phys. Rev. Lett. **70**, 2237 (1993).

TABLES

TABLE I. Parameters and constants of the Tucson-Melbourne three-nucleon potential.

Parameter	Value	
a	1.13	μ^{-1}
b	-2.58	μ^{-3}
c	1.00	μ^{-3}
d	-0.753	μ^{-3}
m	938.92	MeV
M	1232	MeV
μ	139.6	MeV
m_ρ	768.3	MeV
g	$\sqrt{179.7}$	
g_ρ	5.3	
κ_ρ	6.6	
g^*	1.82	μ^{-1}
$G^*_{M\rho}F_{\rho N\Delta}(0)$	14.7	
$\Lambda_{\pi NN}$	5.8	μ
$\Lambda_{\pi N\Delta}$	5.8	μ
$\Lambda_{\rho NN_D}$	12.0	μ
$\Lambda_{\rho NN_P}$	7.4	μ
$\Lambda_{\rho N\Delta}$	5.8	μ

TABLE II. Triton binding energies in MeV calculated for different combinations of two-nucleon and three-nucleon potentials. The column labeled "no 3NP" shows the results when no three-nucleon potential is included. The parameter set of Table I is employed.

	no 3NP	$\pi\pi$	$\pi\pi+\pi\rho$	$\pi\pi+\pi\rho+\rho\rho$
RSC	-7.229	-8.904	-8.438	-8.451
Paris	-7.381	-9.060	-8.486	-8.494
Nijmegen	-7.537	-9.347	-8.692	-8.689
OBEPQ	-8.315	-11.056	-9.639	-9.596

TABLE III. Triton binding energies in MeV calculated for various cut-off parameters in the employed three-nucleon potentials. For the ρ-baryon-baryon vertices, the set of cut-off parameters of Table I is labeled as "soft", whereas the choice $\Lambda_{\rho NN_D} = \Lambda_{\rho NN_P} = \Lambda_{\rho N\Delta} = 13.4\mu$ is referred to as "hard", thereby characterizing the corresponding vertex form factors. The Paris potential was taken as two-nucleon potential.

		$\Lambda_{\pi NN}$	
three-nucleon potential	4.1μ	5.8μ	7.1μ
$\pi\pi$	-7.543	-9.060	-12.313
$\pi\pi + \pi\rho$ soft	-7.409	-8.486	-10.558
$\pi\pi + \pi\rho$ hard	-7.484	-8.468	-10.583
$\pi\pi + \pi\rho + \rho\rho$ soft	-7.416	-8.494	-10.558
$\pi\pi + \pi\rho + \rho\rho$ hard	-7.468	-8.256	-9.741

TABLE IV. Expectation values of various components of the Tucson-Melbourne three-nucleon potentials, evaluated with the respective wave functions fully correlated by two- and three-nucleon forces. The parameter set of Table I is used in the calculations. In the four columns, the three-nucleon potentials are combined with different two-nucleon potentials. The superscript $(+)$ or $(-)$ indicates the even or odd symmetry of the respective potential component under isospin exchange of two nucleons. In addition, the probabilities of S, S', P, and D waves in the triton wave function in percent and the corresponding binding energy E_T are displayed. The binding energy row E_T is identical to the last column of Table II. All energies are in MeV.

	RSC	Paris	Nijmegen	OBEPQ
$\pi\pi$ [MeV]				
$a^{(+)}$	0.009	-0.005	-0.018	-0.089
$b^{(+)}$	-1.397	-1.331	-1.246	-0.867
$c^{(+)}$	-0.432	-0.661	-0.912	-2.313
$d^{(-)}$	-0.355	-0.322	-0.335	-0.754
total $\pi\pi$	-2.174	-2.319	-2.511	-4.024
$\pi\rho$ [MeV]				
K.R.$^{(-)}$	0.089	0.136	0.171	0.488
$\Delta^{(+)}$	0.169	0.151	0.159	0.319
$\Delta^{(-)}$	0.127	0.165	0.171	0.164
total $\pi\rho$	0.385	0.452	0.501	0.970
$\rho\rho$ [MeV]				
Beg$^{(-)}$	-0.002	0.008	0.017	0.050
$\Delta^{(+)}$	-0.001	-0.010	-0.016	-0.051
$\Delta^{(-)}$	-0.012	-0.008	-0.007	0.000
total $\rho\rho$	-0.014	-0.011	-0.006	-0.001
total 3NP [MeV]	-1.803	-1.878	-2.016	-3.055
E_T [MeV]	-8.451	-8.494	-8.689	-9.596
$P(S)$	88.70	89.92	90.73	92.70
$P(S')$	1.12	1.10	0.90	1.00
$P(P)$	0.16	0.13	0.13	0.10
$P(D)$	10.03	8.84	8.25	6.20

TABLE V. Expectation values of the Tucson-Melbourne three-nucleon potential, split into Δ, σ-term, Z-graph, and "current algebra" contributions. The energies are in MeV.

	RSC	Paris	Nijmegen	OBEPQ
$\pi\pi$ [MeV]				
Δ	-1.08	-1.02	-0.97	-0.92
σ	-0.98	-1.23	-1.50	-3.05
Z	-0.01	0.04	0.07	0.20
ca	-0.12	-0.10	-0.11	-0.24
total 3NP [MeV]				
Δ	-0.79	-0.72	-0.66	-0.49
σ	-0.98	-1.23	-1.50	-3.05
Z	0.08	0.17	0.24	0.69
ca	-0.12	-0.10	-0.09	-0.19

FIGURES

FIG. 1. Feynman diagram for the $\pi\pi$ exchange three-nucleon potential.

FIG. 2. Feynman diagram for the $\pi\rho$ exchange three-nucleon potential.

FIG. 3. Feynman diagram for the $\rho\rho$ exchange three-nucleon potential.

FIG. 4. Dependence of calculated triton binding energies on $\Lambda_{\pi NN}$ for the Tucson-Melbourne three-nucleon potential in combination with the Paris potential. The horizontal lines represent the experimental triton binding energy (dotted) and the calculated value without three-nucleon force (long dashed). The triangles are calculated binding energies with the $\pi\pi$ potential, the full (open) circles are binding energies with the full three-nucleon force with soft (hard) ρNN form factors. The lines through the symbols are drawn to guide the eye.

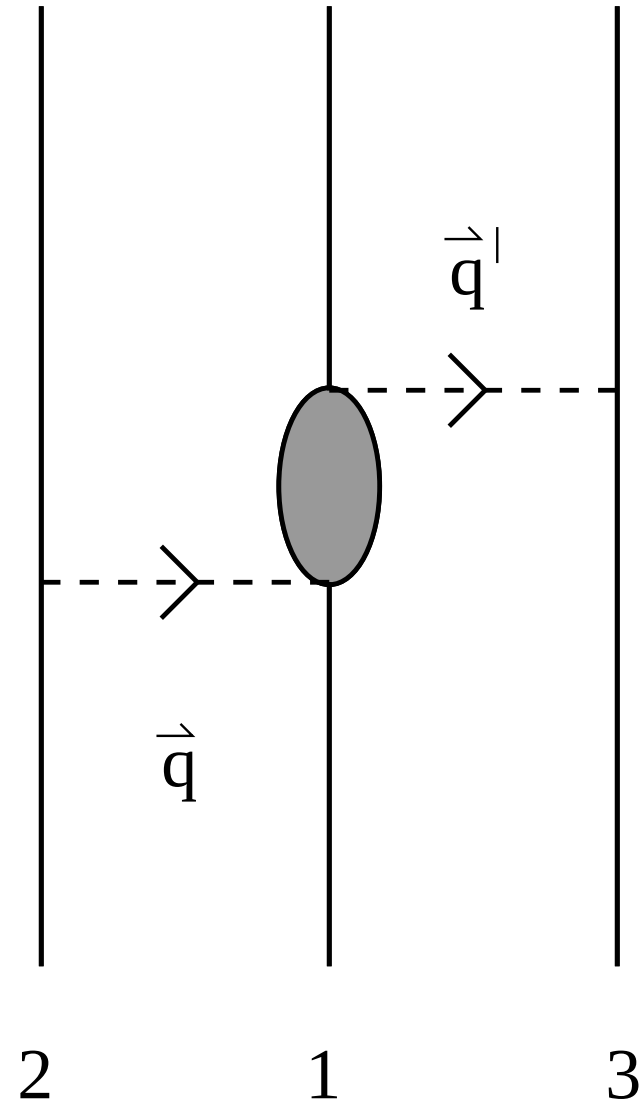


Fig. 1 of: A. Stadler, J. Adam Jr., H. Henning, P.U. Sauer, "Triton calculations with pi- and rho-exchange three-nucleon forces"

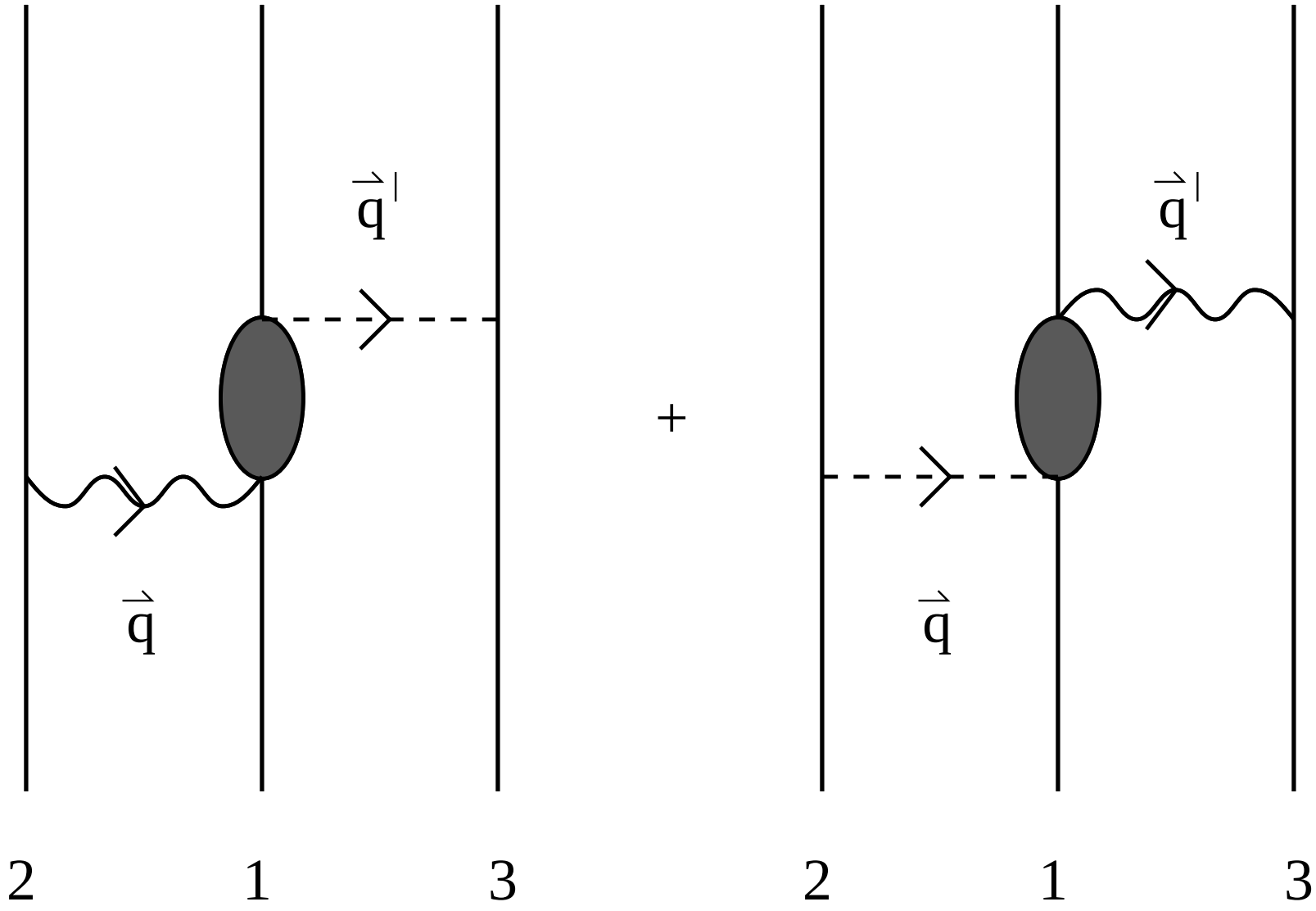


Fig. 2 of: A. Stadler, J. Adam Jr., H. Henning, P.U. Sauer, "Triton calculations with pi- and rho-exchange three-nucleon forces"

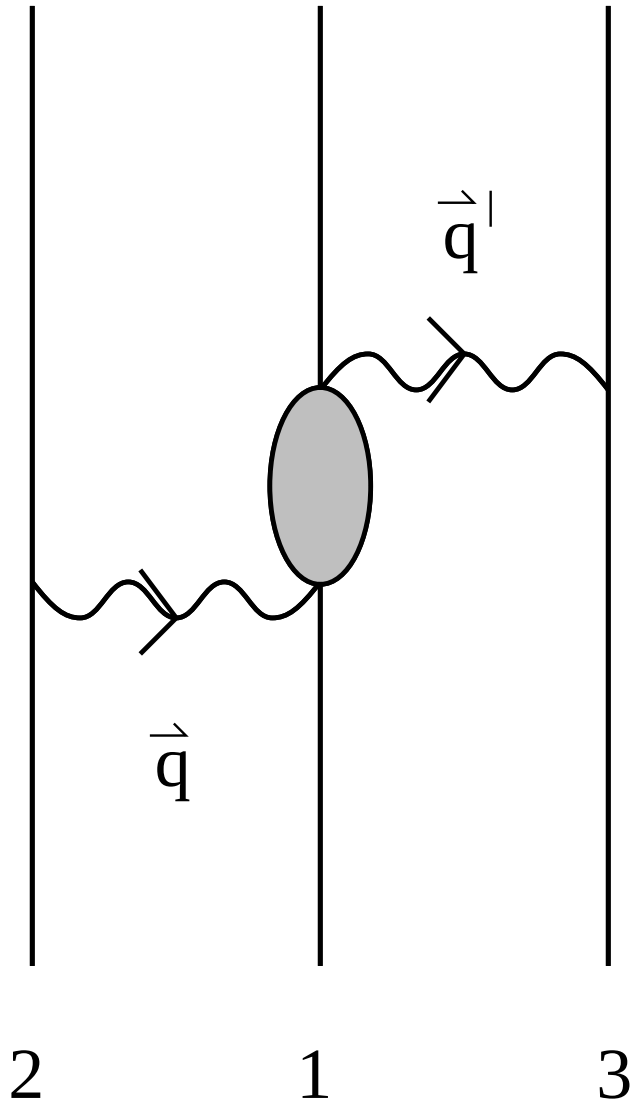


Fig. 3 of: A. Stadler, J. Adam Jr., H. Henning, P.U. Sauer, "Triton calculations with pi- and rho-exchange three-nucleon forces"

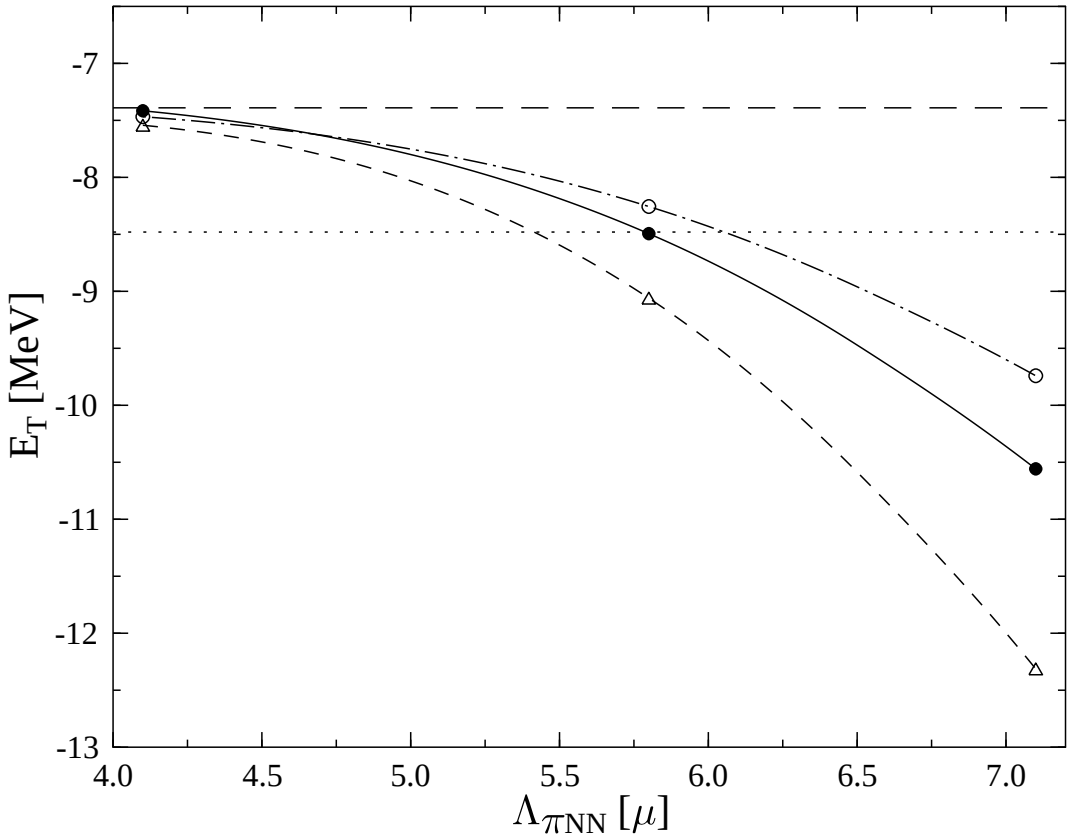


Fig. 4 of: A. Stadler, J. Adam Jr., H. Henning, P.U. Sauer, ‘‘Triton calculations with pi- and rho-exchange three-nucleon forces’’